Exploring the Emergent Redox Chemistry of Pd(II) Nodes with Pendant Ferrocenes: from Precursors, through Building Blocks, to Self-Assemblies

Austin B. Gilbert, Matthew R. Crawley, Trevor J. Higgins, Yuguang C. Li, David F. Watson*, Timothy R. Cook*

Department of Chemistry, University at Buffalo the State University of New York, Buffalo, New York 14260, United States

Supporting Information

Spectroscopic, electrochemical, and spectroelectrochemical characterization

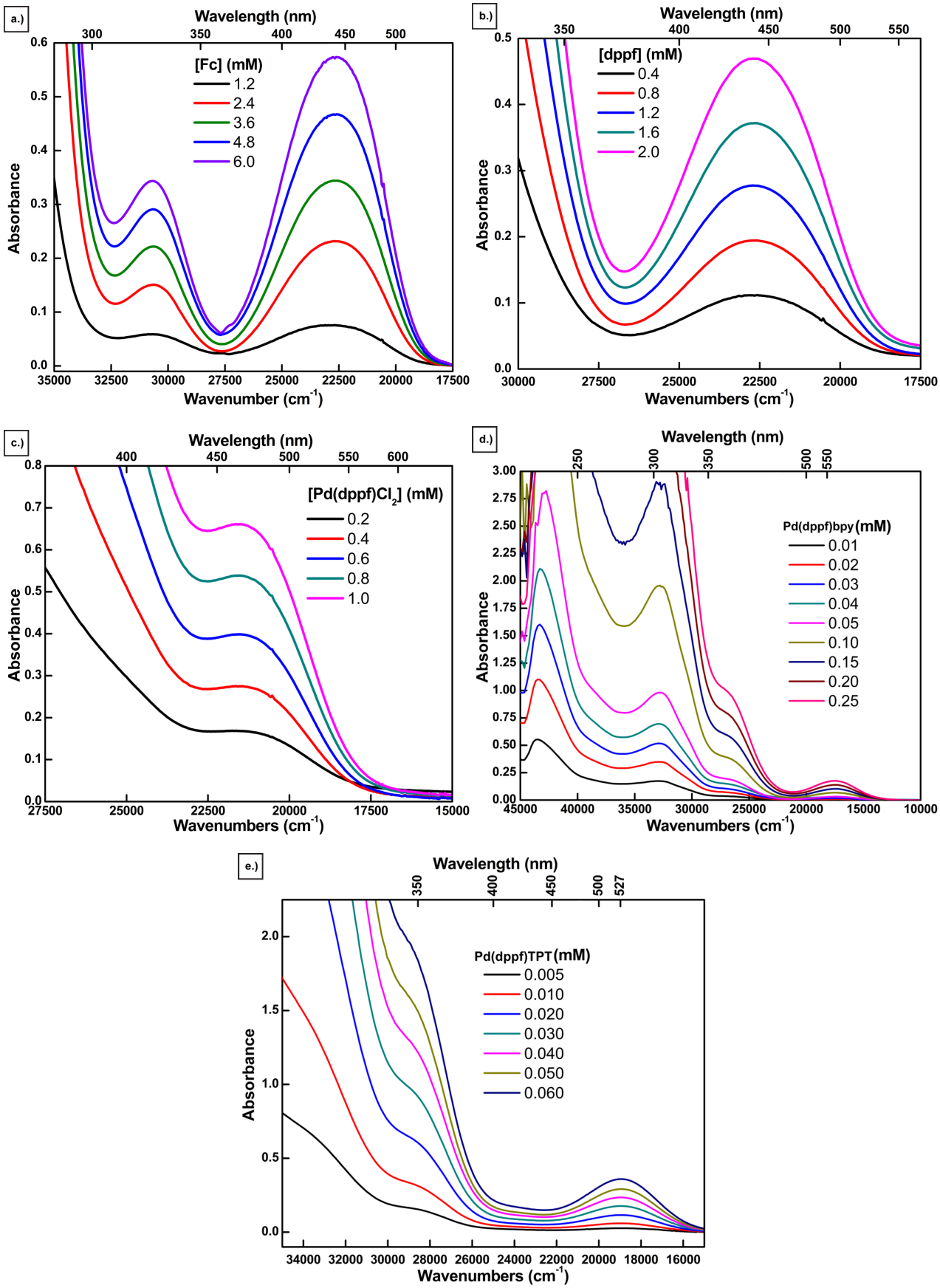

Figure S1: UV-Vis absorbance spectra of a.) **Fc**, b.) **dppf**, c.) **Pd(dppf)Cl2**, d.) **Pd(dppf)bpy**, e.) **Pd(dppf)TPT**. All spectra were acquired at the specified sample concentration in dry DCM.

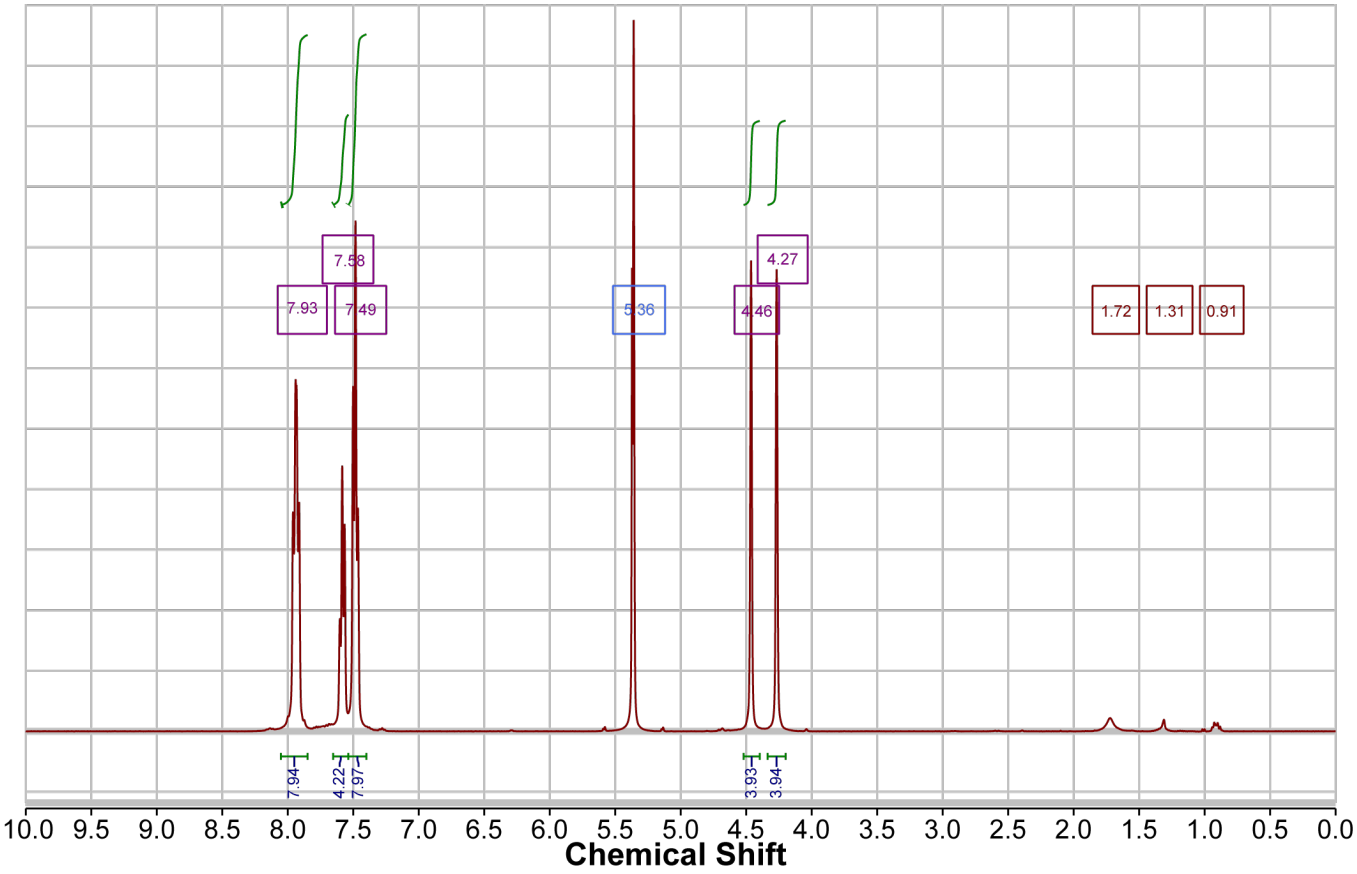

Figure S2: ^{1}H-NMR spectrum of **Pd(dppf)Cl$_2$** acquired in D_2-DCM.

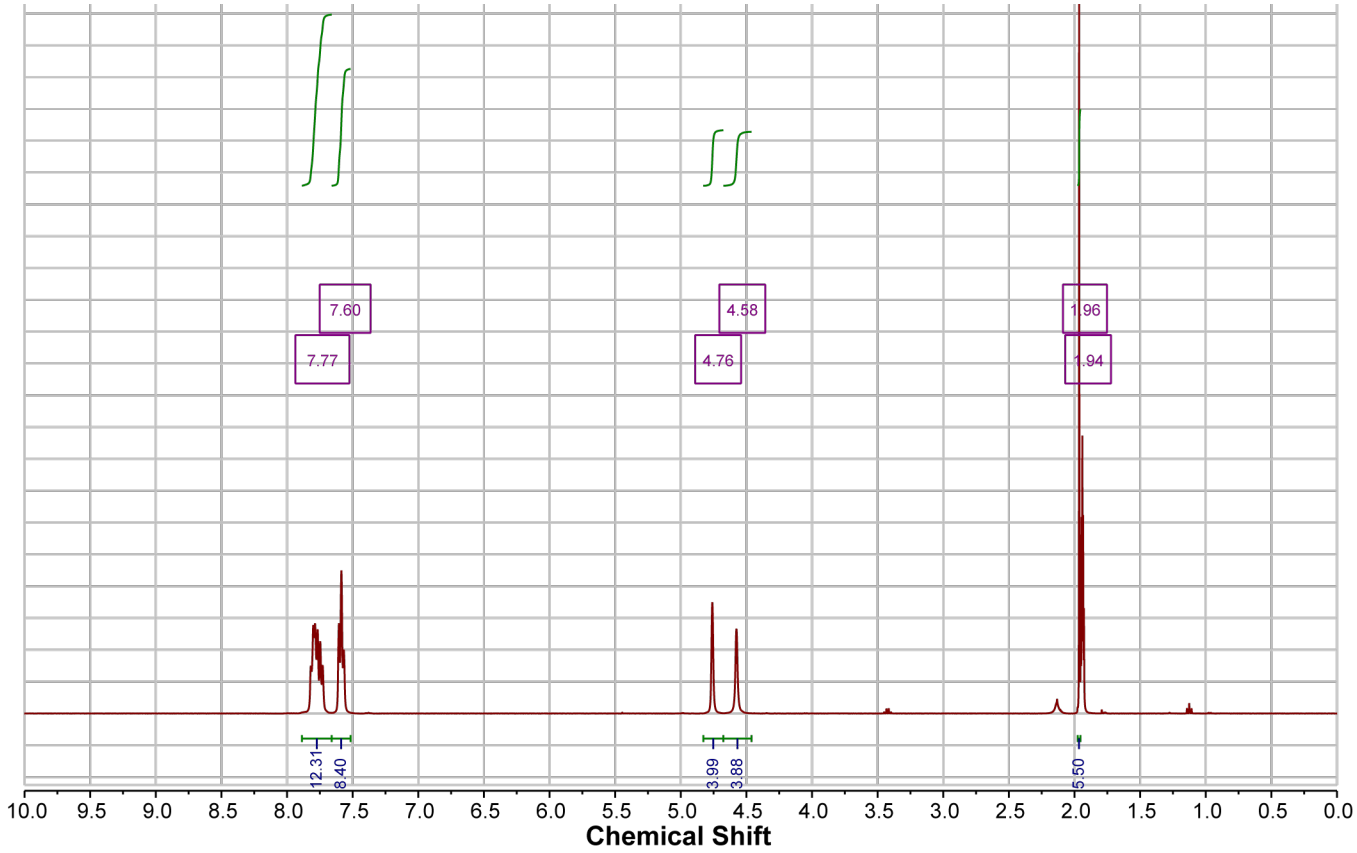

Figure S3: ^{1}H-NMR spectrum of $[Pd(dppf)(ACN)_2](PF_6)_2$ acquired in D_2-DCM.

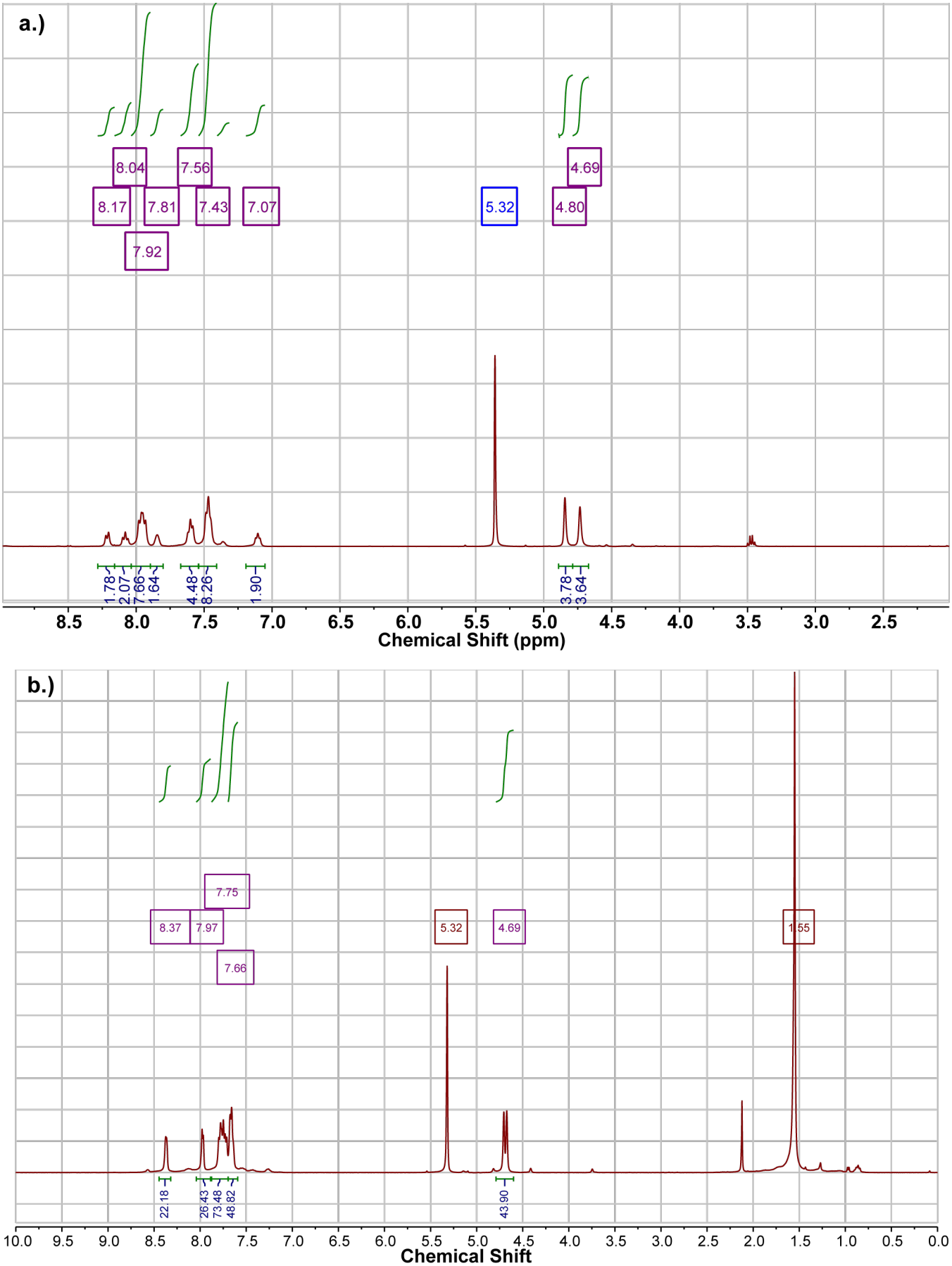

Figure S4: ^{1}H-NMR spectra of a.) **Pd(dppf)bpy** and b.) **Pd(dppf)TPT** acquired in D_2-DCM.

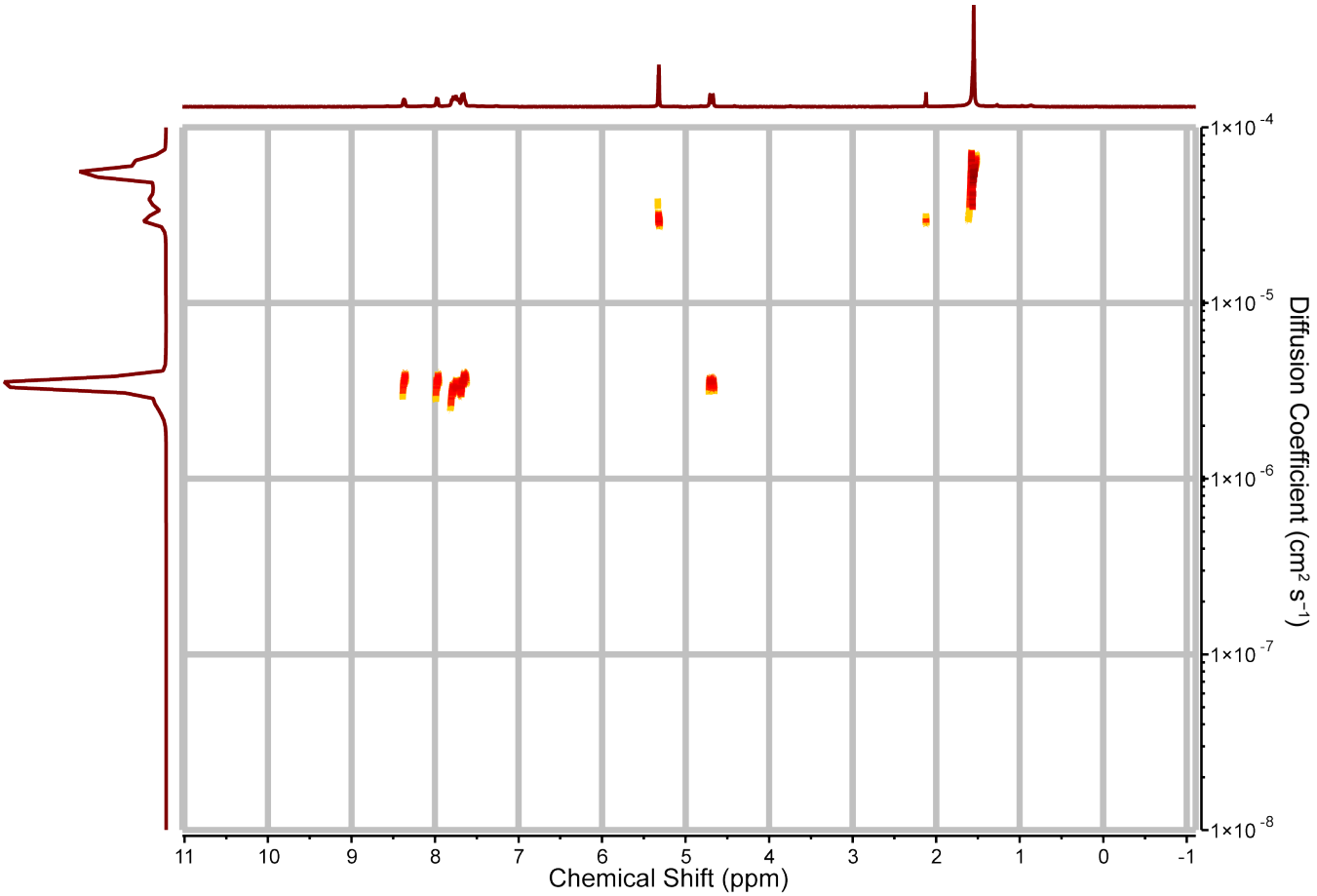

Figure S5: ^{1}H-DOSY NMR spectrum of **Pd(dppf)TPT** acquired in D_2-DCM.

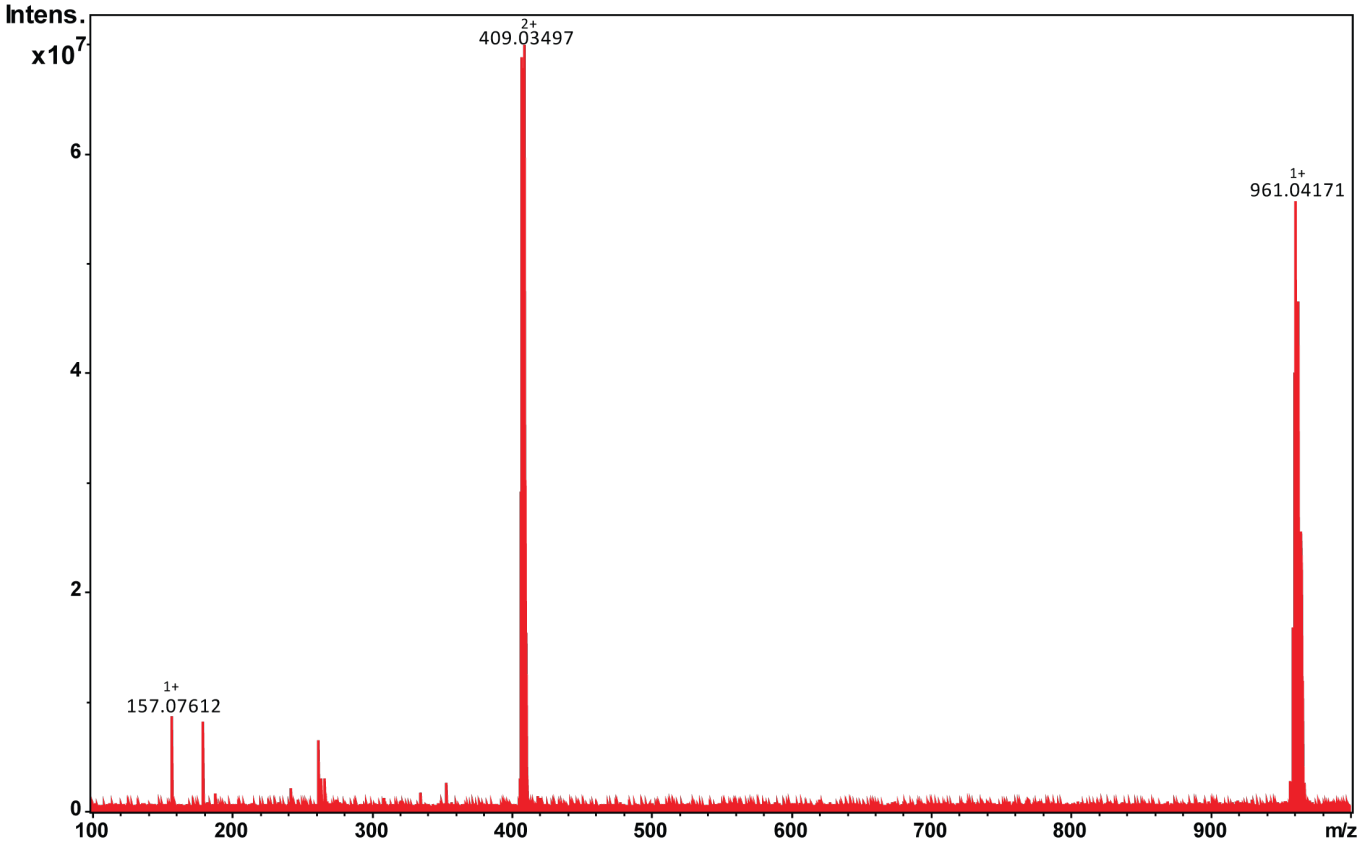

Figure S6: Full ESI-FT-ICR MS of **Pd(dppf)bpy** acquired from a solution in DCM.

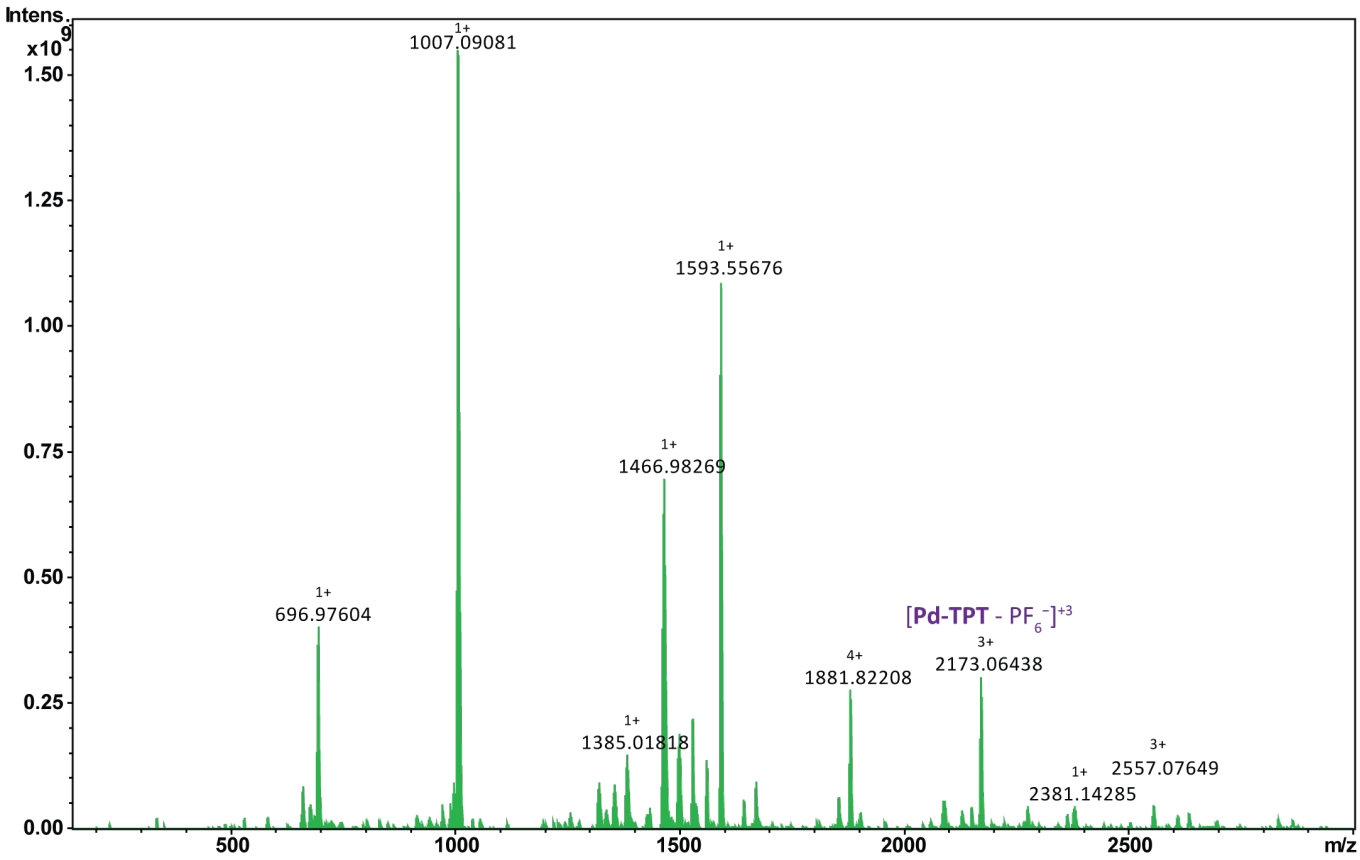

Figure S7: Full ESI-FT-ICR MS of **Pd(dppf)TPT** acquired from a solution in DCM.

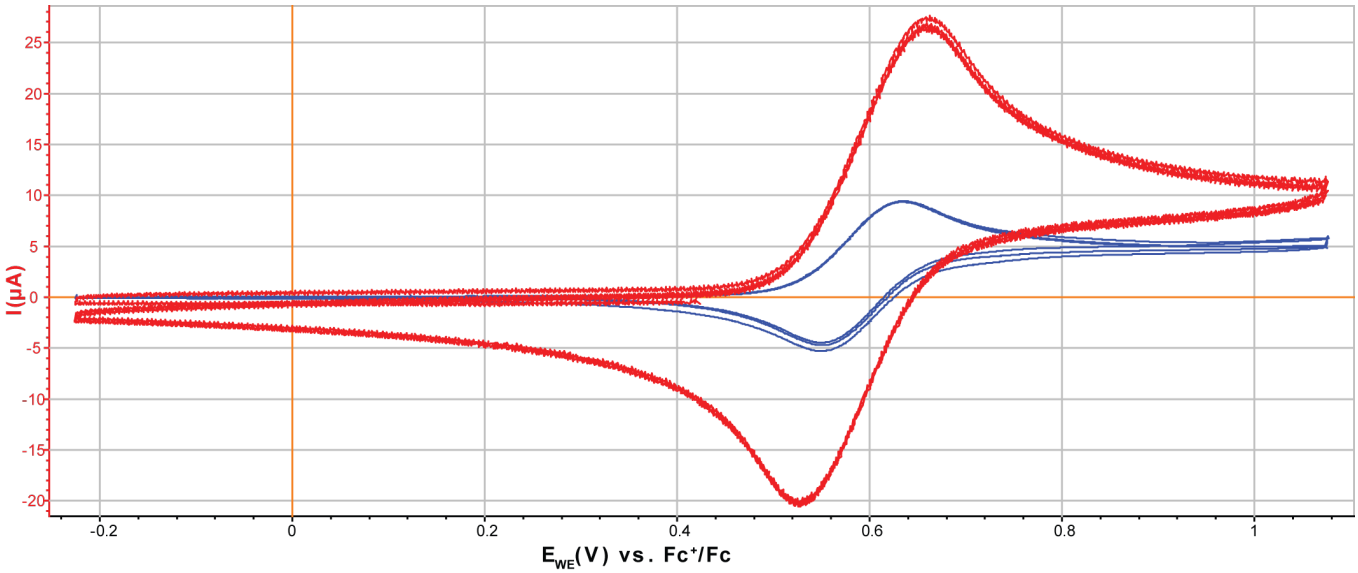

Figure S8: Cyclic voltammograms of $Pd(dppf)Cl_2$ (1.00 mM). Fc-centered oxidation event at scan rates of 100 mV s^{-1} (red) and 10 mV s^{-1} (blue). Shown are 3 cycles starting from E_{oc} in DCM (100 mM $TBAPF_6$).

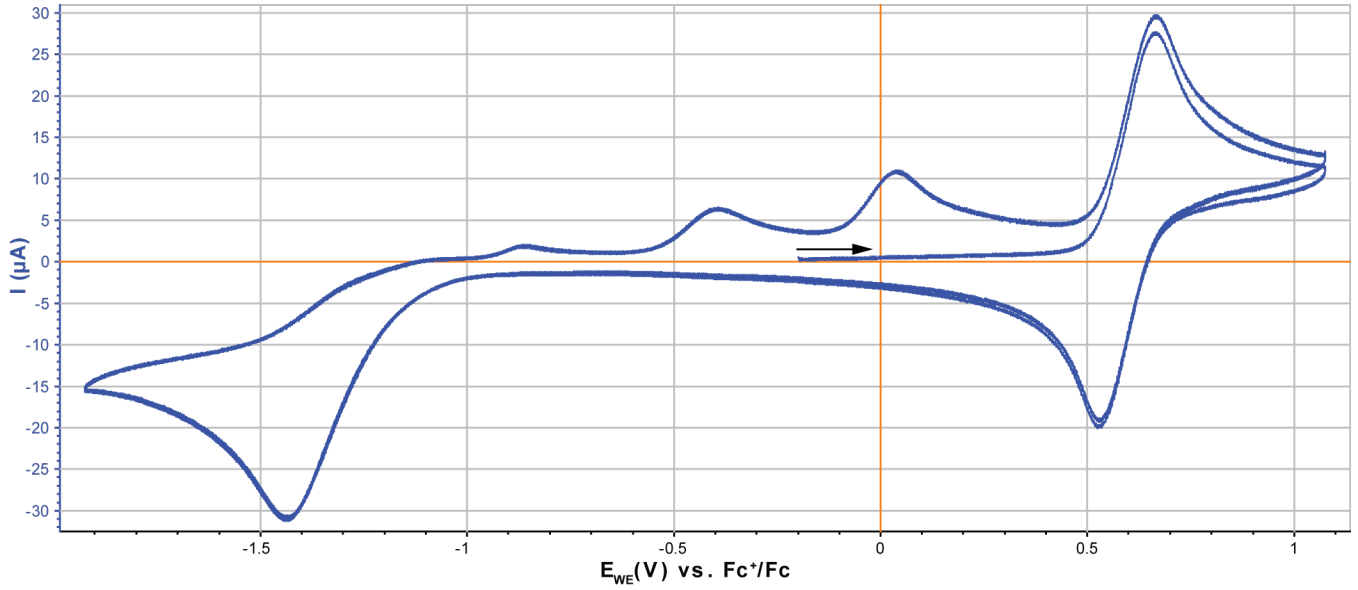

Figure S9: Cyclic voltammograms of **$Pd(dppf)Cl_2$** (1.00 mM). Shown are 3 cycles starting from E_{oc} at 100 mV/s in DCM (100 mM $TBAPF_6$).

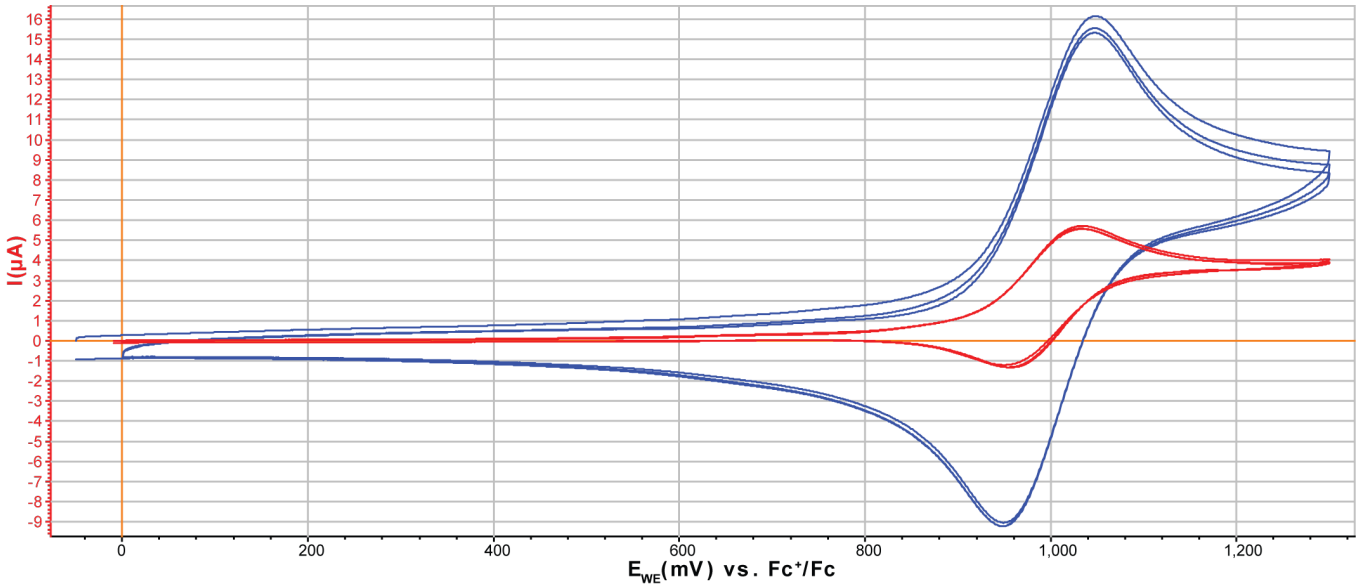

Figure S10: Cyclic voltammograms of **Pd(dppf)bpy** (1.80 mM) Fc-centered oxidation event at scan rates of 100 mV s^{-1} (blue) and 10 mV s^{-1} (red). Shown are 3 cycles starting from E_{oc} in DCM (100 mM $TBAPF_6$).

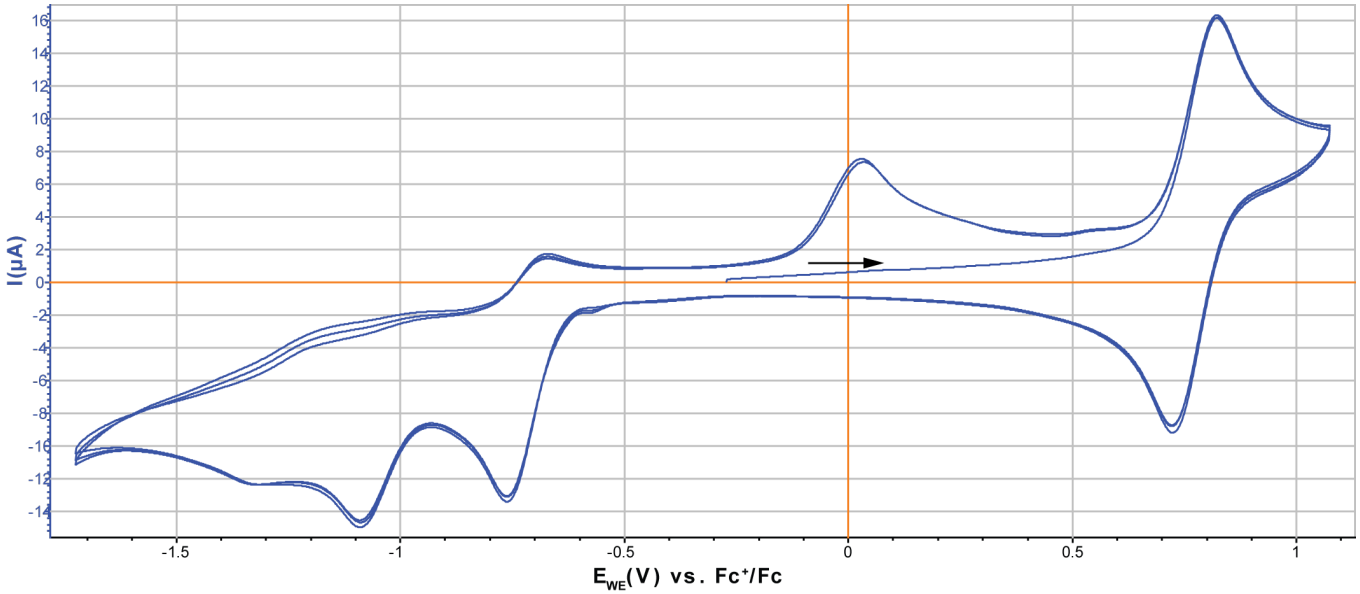

Figure S11: Cyclic voltammograms of **Pd(dppf)bpy** (1.80 mM). Shown are 3 cycles starting from E_{oc} at 100 mV/s in DCM (100 mM $TBAPF_6$).

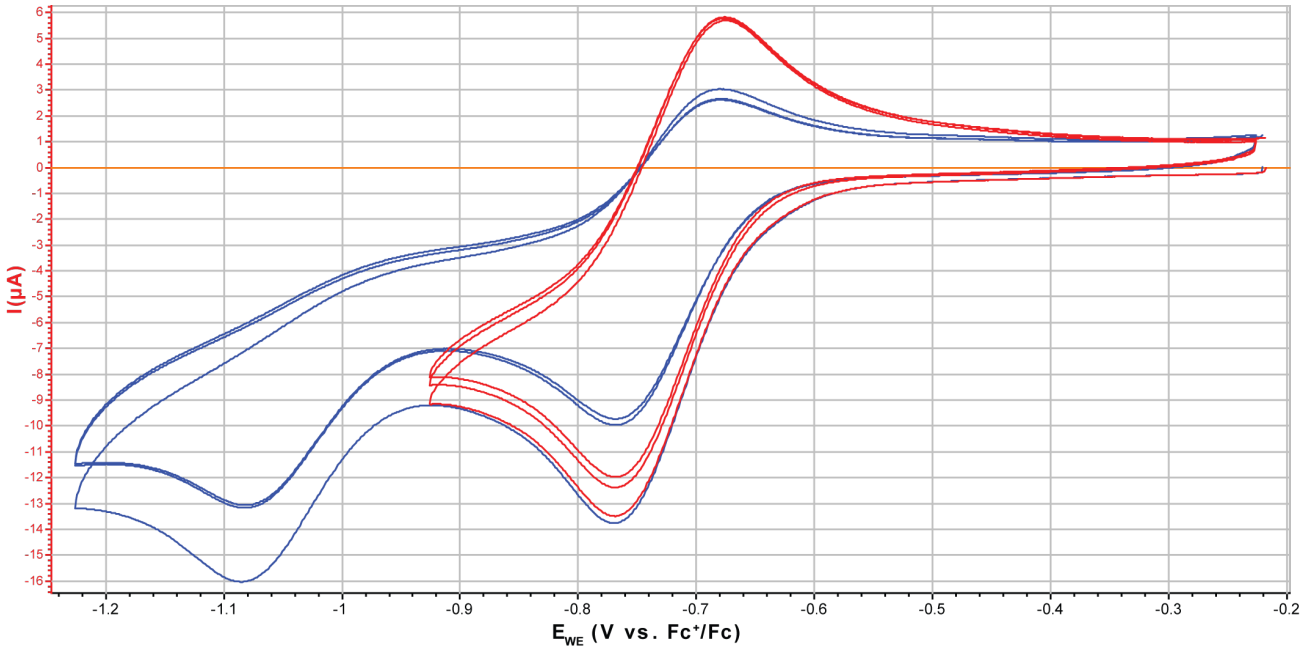

Figure S12: Cyclic voltammograms of **Pd(dppf)bpy** reduction events with varying potential windows. Shown are 3 cycles starting from E_{oc} at 100 mV/s in DCM (100 mM $TBAPF_6$).

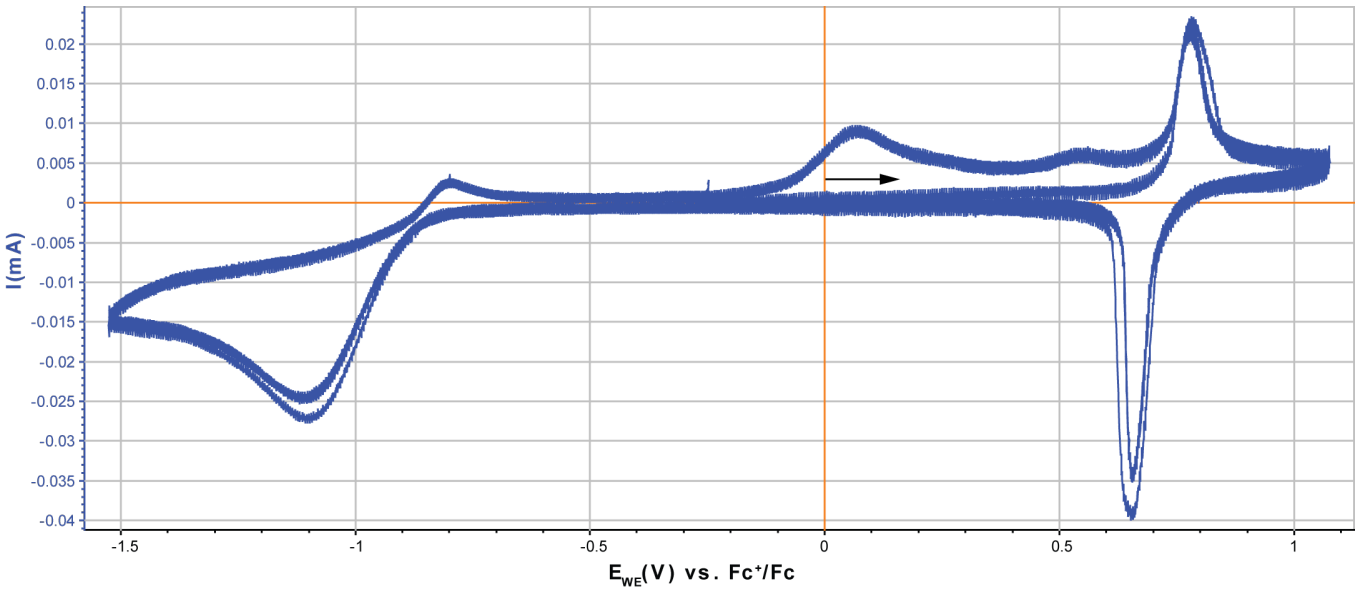

Figure S13: Cyclic voltammograms of **Pd(dppf)TPT** (0.30 mM). Shown are 3 cycles starting from E_{oc} at 100 mV/s in DCM (100 mM $TBAPF_6$).

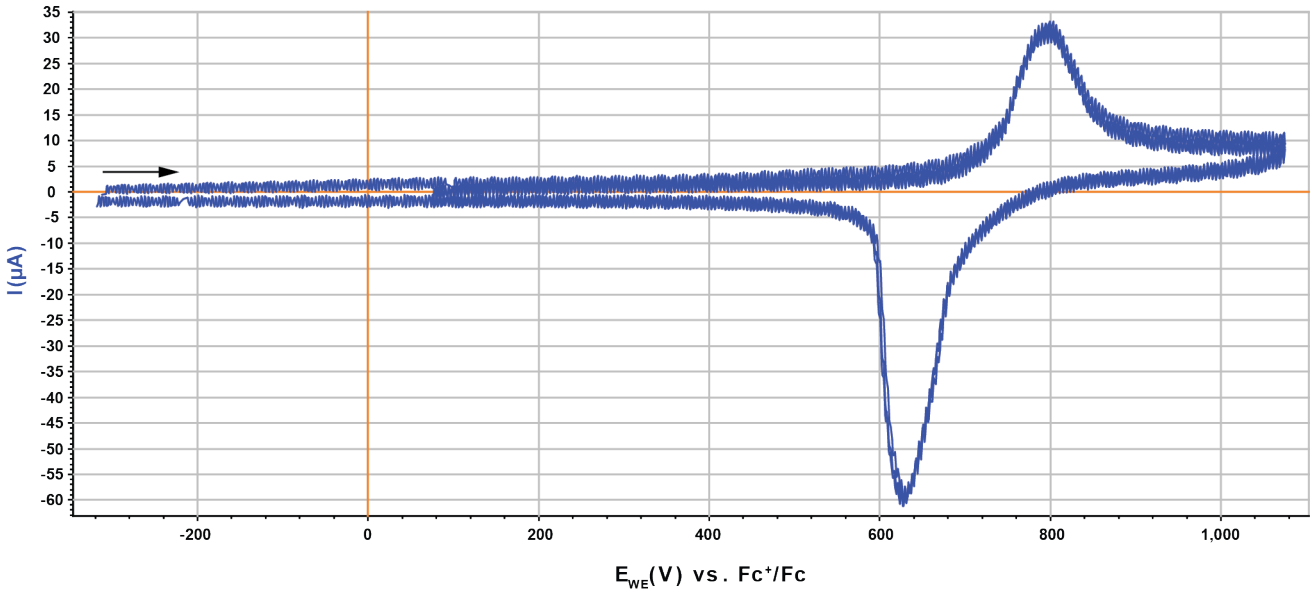

Figure S14: Cyclic voltammograms of **Pd(dppf)TPT** (0.30 mM). Shown are 3 cycles starting from E_{oc} at 250 mV/s in DCM (100 mM $TBAPF_6$).

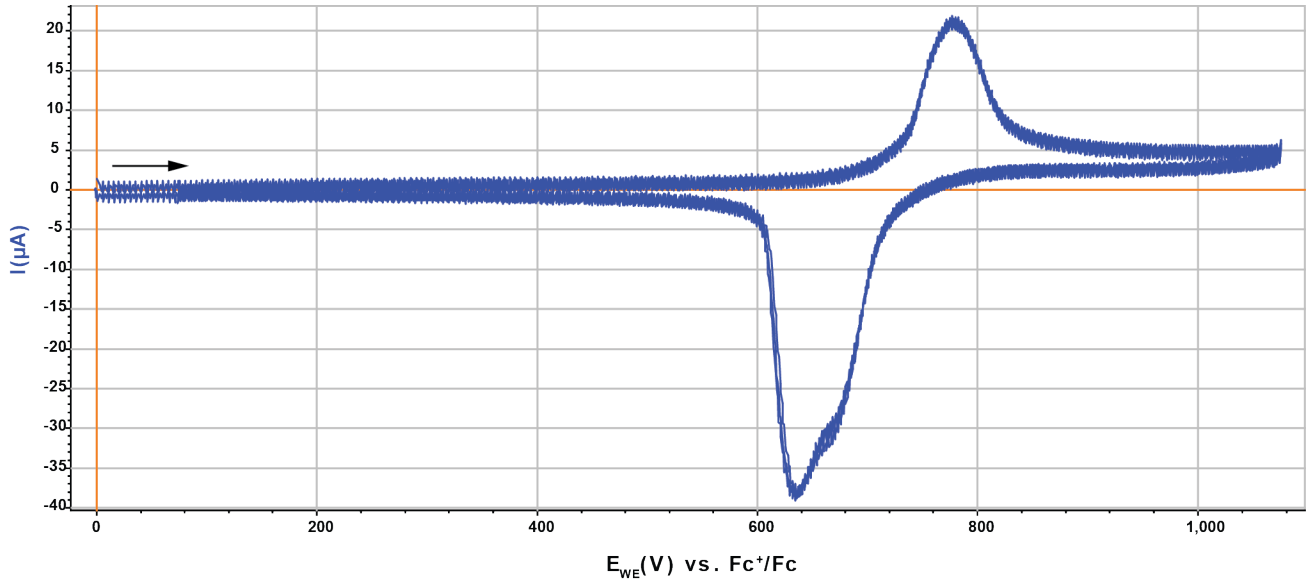

Figure S15: Cyclic voltammograms of **Pd(dppf)TPT** (0.30 mM). Shown are 3 cycles starting from E_{oc} at 100 mV/s in DCM (100 mM $TBAPF_6$).

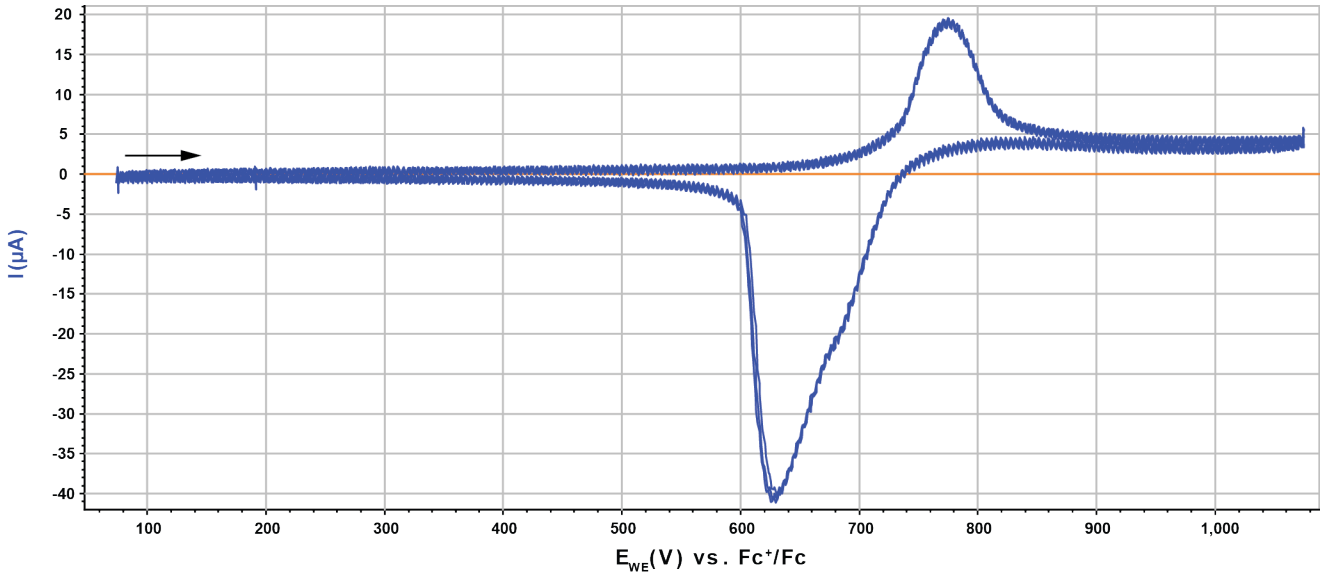

Figure S16: Cyclic voltammograms of **Pd(dppf)TPT** (0.30 mM). Shown are 3 cycles starting from E_{oc} at 80 mV/s in DCM (100 mM $TBAPF_6$).

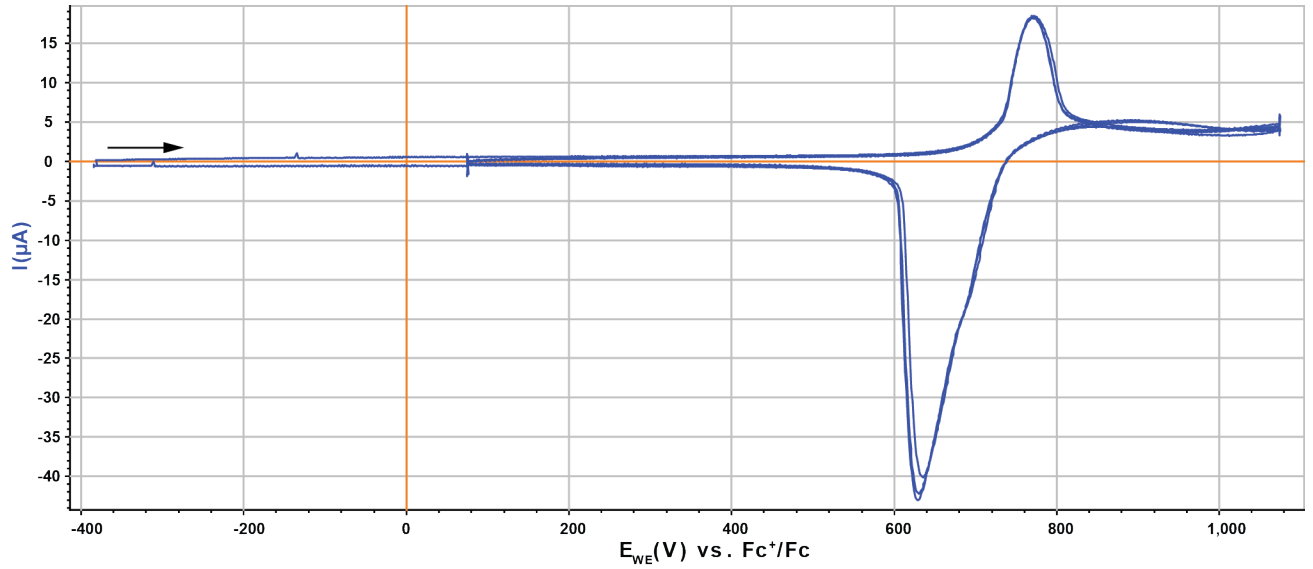

Figure S17: Cyclic voltammograms of **Pd(dppf)TPT** (0.30 mM). Shown are 3 cycles starting from E_{oc} at 60 mV/s in DCM (100 mM $TBAPF_6$).

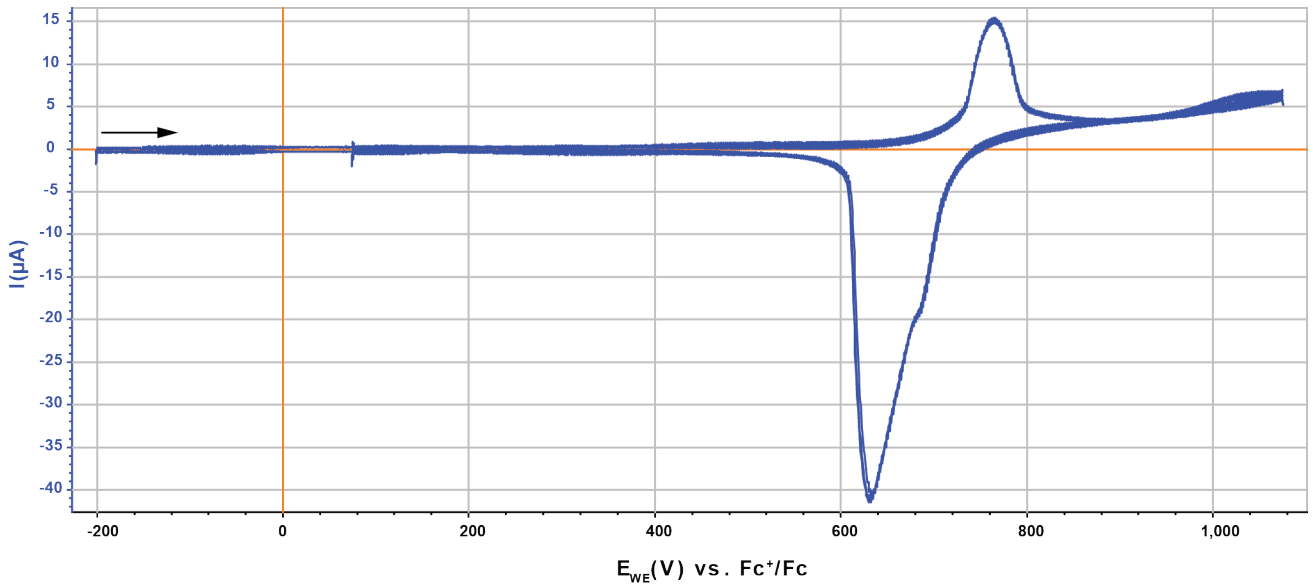

Figure S18: Cyclic voltammograms of **Pd(dppf)TPT** (0.30 mM). Shown are 3 cycles starting from E_{oc} at 40 mV/s in DCM (100 mM $TBAPF_6$).

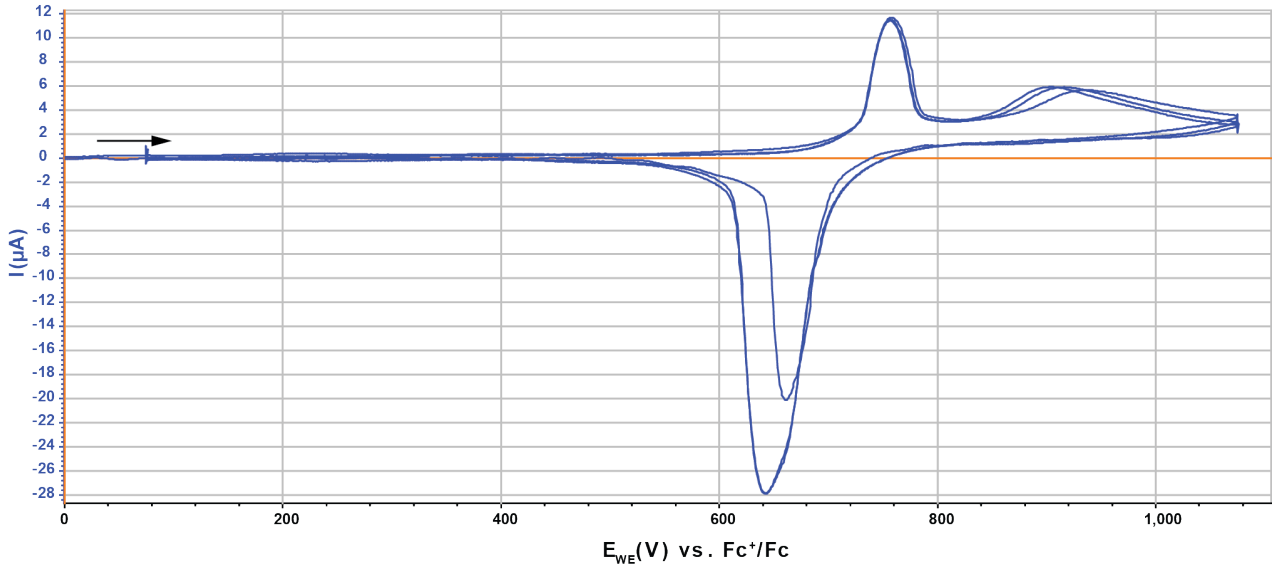

Figure S19: Cyclic voltammograms of **Pd(dppf)TPT** (0.30 mM). Shown are 3 cycles starting from E_{oc} at 20 mV/s in DCM (100 mM $TBAPF_6$).

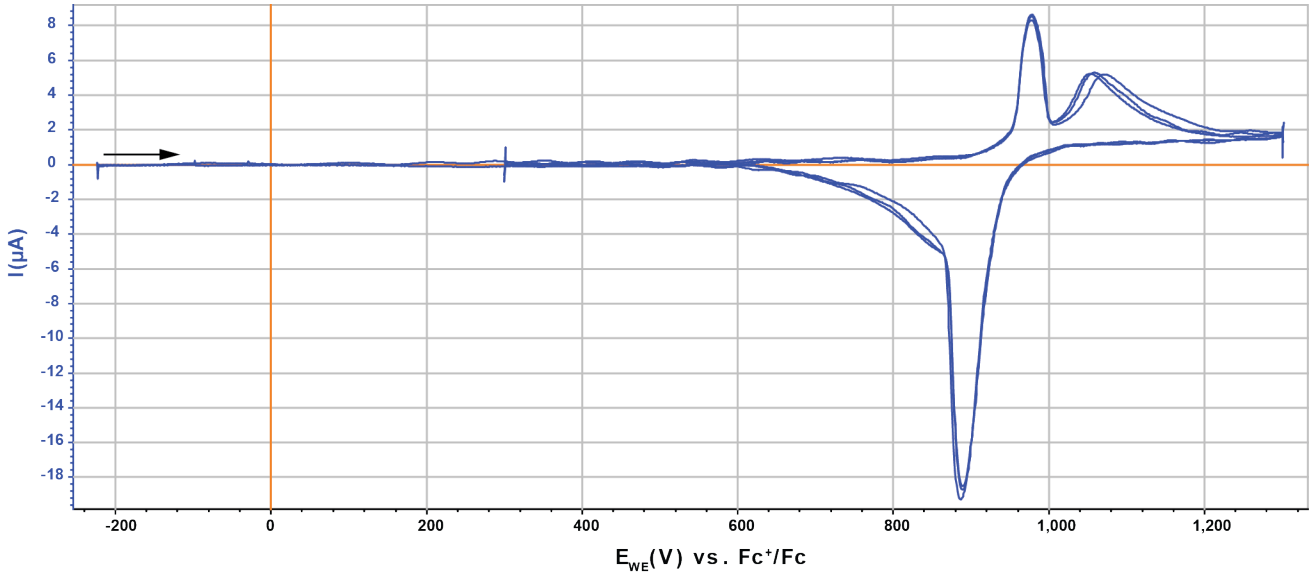

Figure S20: Cyclic voltammograms of **Pd(dppf)TPT** (0.30 mM). Shown are 3 cycles starting from E_{oc} at 10 mV/s in DCM (100 mM $TBAPF_6$).

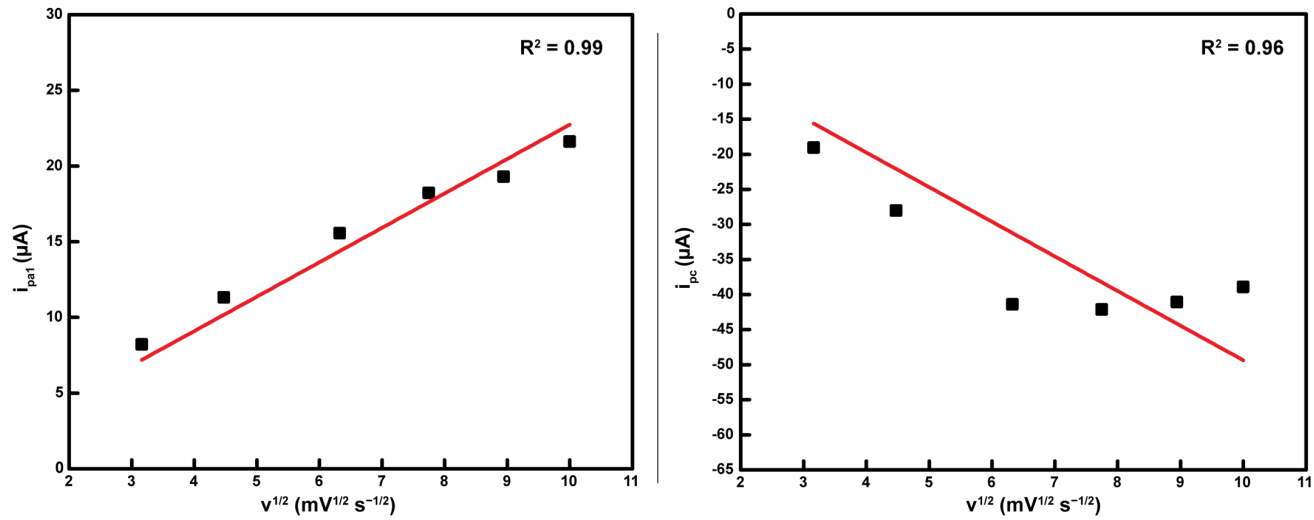

Figure S21: Relationship between peak current (i) and the square root of scan rate ($v^{1/2}$) from cyclic voltammograms of 0.30 mM **Pd(dppf)TPT** in DCM (100 mM $TBAPF_6$) for the first anodic peak (left) and the cathodic peak (right). Linear fits are shown in red.

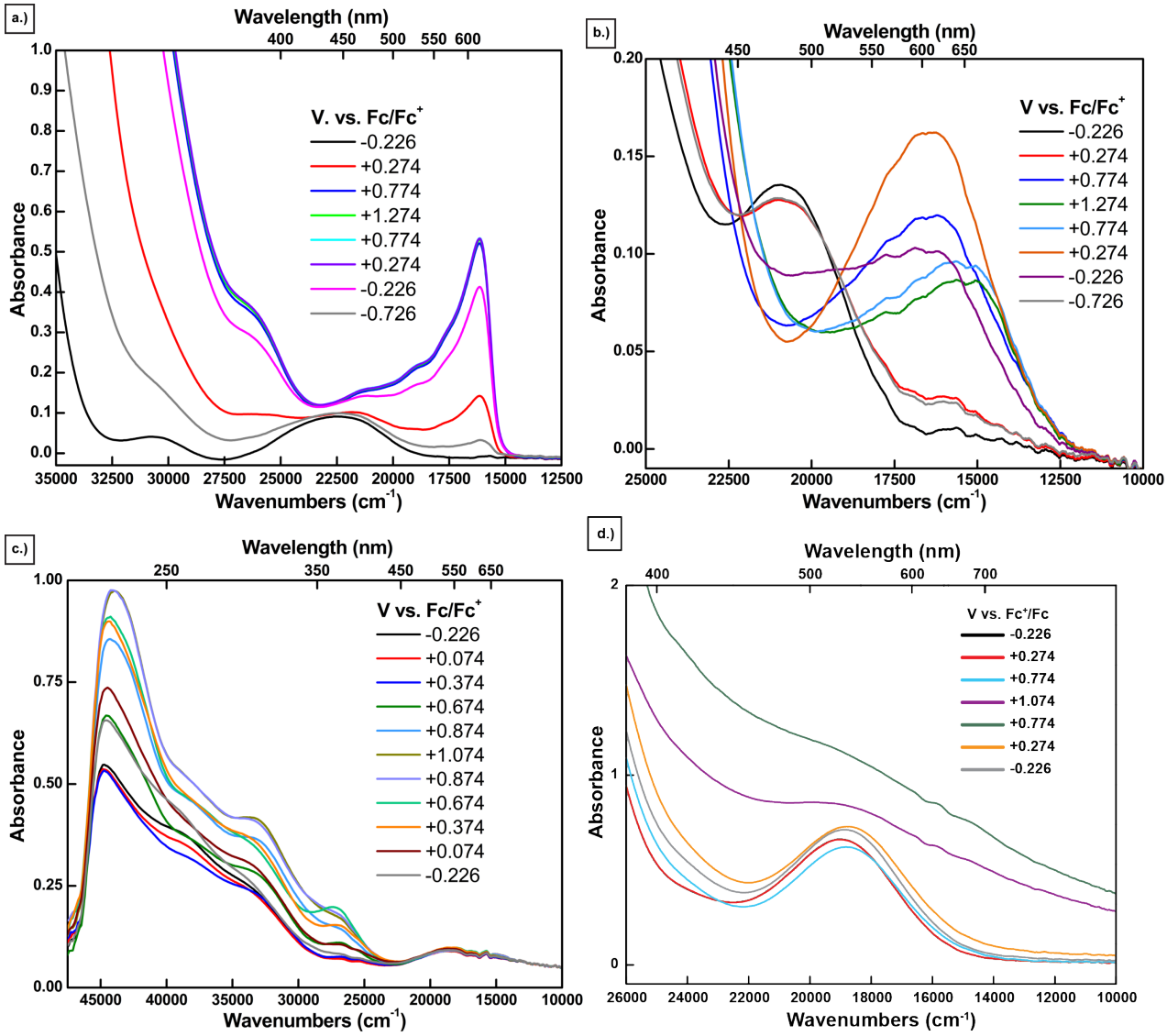

Figure S22: UV-Vis absorbance spectra acquired from spectroelectrochemical experiments probing the Fc-centered oxidation events of a.) **Fc** (1.8 mM), b.) **Pd(dppf)Cl$_2$** (1.8 mM), c.) **Pd(dppf)TPT** (0.04 mM), and d.) **Pd(dppf)TPT** (0.30 mM). All solutions were prepared in dry DCM (100 mM TBAPF$_6$).

Figure S23: Photographs of FTO working electrode used in diffuse reflectance spectroelectrochemical experiments. The FTO films shown are following: (1) the bulk oxidation and deposition of **Pd(dppf)TPT** (left), and (2) the subsequent bulk rereduction of the **Pd(dppf)TPT**-modified film (right).